PNAS
www.pnas.org

Supplementary Information for

Regulation of *CCL2* expression in human vascular endothelial cells by a neighboring divergently transcribed long noncoding RNA.

Nadiya Khyzha[1-3], Melvin Khor[1-3], Peter DiStefano[1-3], Liangxi Wang[4,5], Ljubica Matic[6], Ulf Hedin[6], Michael D. Wilson[4,5], Lars Maegdefessel[6,7], Jason E. Fish[1-3]

Jason E. Fish

jason.fish@utoronto.ca

This PDF file includes:

Supplemental Methods

Captions for figures

Figures S1 to S13

Tables S1 to S5

References for SI reference citations

Other supplementary materials for this manuscript include the following:

Datasets S1 to S7

www.pnas.org/cgi/doi/10.1073/pnas.1904108116

Supplemental Methods

Nuclear Cytoplasmic Fractionation:

HMEC cell pellets ($3x10^6$ cells) were collected and washed twice in ice cold PBS (-/-). The final PBS wash was performed in 1 mL of PBS at 800g for 5 min. Cells were lysed for 5 minutes on ice in the lysis solution (50 mM Tris-HCl, pH 8.0; 140 mM NaCl; 1.5 mM $MgCl_2$, 0.5% Nonidet P-40; 0.2 units/ µl RNaseOUT; 1mM dithiothreitol (DTT)). Nuclei were pelleted by spinning at 300g for 2 min. The supernatant cytoplasmic fraction was removed and the nuclear pellet was washed in 500 µl of PBS for 5 min at 300g. TRIzol Reagent (Thermo Fisher Scientific) was then added to the cytoplasmic and nuclear fractions. RNA was isolated and equal volumes of RNA from each fraction were used to make cDNA.

Chromatin Immunoprecipitation followed by sequencing (ChIP-seq) analysis:

ChIP-seq analysis was performed on previously published data (GSE89970) (1) ("SI Appendix, Table S6"). The quality of reads was analyzed using FASTQC (2) and the Illumina adapter sequences along with low quality base pairs (Phred <20) were trimmed off using Trim Galore!. The reads were than aligned to hg19 with Bowtie2 using the sensitive end-to-end pre-set option (-D 15 -R 2 -L 22 -I S,1,1.5) (3). Alignment quality was than assessed as per ENCODE guideline metrics using the “qualityScores_EM” and “getCrossCorrelationScores” functions from the “ChIC” Bioconductor package ("SI Appendix, Table S6"). Afterwards, peaks were called using MACS2 (3, 4). BAM files from replicate experiments were merged into one BAM file using BamTools (5). Profile plots were generated using ComputeMatrix (DeepTools2) and PlotProfile (DeepTools2) (6) over the given genomic coordinates that corresponded to the coordinates

between the mRNA-lncRNA pairs. For visualization, bamCoverage (DeepTools2)(6) was used to normalize reads based on RPKM and to generate BigWig files.

Mass Spectrometry Analysis:

Mass spectrometry and all sample preparation was performed by SPARC Molecular Analysis, The Hospital for Sick Children, Toronto, Canada. Samples were resuspended in 50 µL of 50 mM NH_4HCO_3 (pH=8.3), and DTT was added to reduce cysteines at a final concentration of 10 mM. Cysteines were reduced at 60°C for 1 hour. Samples were cooled to room temperature and iodoacetamide was added to a final volume of 20 mM. Samples were incubated at room temperature in the dark for 30 minutes. Iodoacetamide was then inactivated by adding DTT to a final concentration of 40 mM. TPCK-treated trypsin (Promega), was added to a final protease:protein ration of 1:50-1:100 and samples were digested overnight at 37^{o}C. Magnetic beads were removed, samples were lyophilized, resuspended in 1% TFA and the free digests were combined. Peptides were purified by homemade C18 tips, and then lyophilized.

Samples were analyzed on a Thermo Scientific Orbitrap Fusion-Lumos Tribid Mass Spectrometer (ThermoFisher, San Jose, CA) outfitted with a nanospray source and EASY-nLC 1200 nano-LC system (ThermoFisher, San Jose, CA) and equipped with ETD mode. Lyophilized peptide mixtures were dissolved in 0.1% formic acid and loaded onto a 75 µm x 50 cm PepMax RSLC EASY-Spray column filled with 2 µM C18 beads (ThermoFisher San, Jose CA) at a pressure of 900 Bar and a temperature of 60^{o}C. Peptides were eluted over 60 minutes at a rate of 250 nL/min using a gradient set up as follows, where Buffer A is 0.1% Formic acid and Buffer B is 80% Acetonitrie, 0.1% Formic Acid, all v/v in HPLC grade water.

Time	Duration	% B
0	0	0
48	48	42
50	2	100
60	2	100

Data was acquired using the FT-FT method. MS1 acquisition was performed with a scan range of 400 m/z - 1600 m/z with resolution set to 120 000, maximum injection time of 120 ms and AGC target set to 4e5. Isolation for MS2 scans was performed in the quadrupole, with an isolation window of 1.6. MS2 scans were done in the orbitrap with a maximum injection time of 100 ms and an AGC target of 5e5. Ions were selected for HCD fragmentation at with a collision energy of 30. The dynamic exclusion was applied using a maximum exclusion list of 500 with one an exclusion duration of 8 s.

RNA Immunoprecipitation (RIP):

RNA Immunoprecipitation was performed as previously described (7). The pull-downs were performed on nuclear extracts from IL-1β stimulated HMEC-1 cells ($5x10^6$ cells per condition). Antibodies used for pull-down included RELA (Cell Signalling 8242S, 5 µg), p300 (Santa Cruz, sc-585, 5 µg), BRD4 (Bethyl Laboratories, A301-985A50, 5 µg), CHD4 (Abcam, ab70467, 5 µg), HNRNPU (Santa Cruz, sc-32315, 5 µg), and IGF2BP2 (Proteintech, 11601-1-AP, 5 µg). As control mouse IgG (Santa Cruz, sc-2025, 5 µg) or rabbit IgG (Santa Cruz, sc-2027, 5 µg) were used.

Western Blotting:

Western Blotting was performed using the following primary antibodies: HNRNPU (Santa Cruz, sc-32315, 1:200) and IGF2BP2 (Proteintech, 11601-1-AP, 1:2000). The secondary antibodies used were anti-mouse IgG HRP conjugated (Cell Signalling, 7076S, 1:3000) and anti-rabbit IgG HRP conjugated (Cell Signalling, 7074S, 1:3000). Protein bands were visualized using the SuperSignal West Pico Plus Chemiluminescent Substrate (Thermo Scientific) using GelCapture Chemi (FroggaBio, MicroChemi 4.2). Silver staining was performed using the Pierce Silver Stain Kit (Thermo Scientific) as per manufacturer's instructions.

Human material analyses:

Patients undergoing surgery for high-grade (>50% **N**orth **A**merican **S**ymptomatic **C**arotid **E**ndarterectomy **T**rial, NASCET) (8) carotid stenosis at the Department of Vascular Surgery, Karolinska University Hospital, Stockholm, Sweden were consecutively enrolled in the study and clinical data recorded on admission. Carotid endarterectomies (carotid plaques) were collected at surgery and retained within the **Bi**obank of **K**arolinska **E**ndarterectomies (BiKE). The BiKE study cohort demographics, details of sample collection, processing and large-scale analyses (transcriptomic profiling) were as previously described in detail (9). Normal artery controls were nine macroscopically disease-free iliac arteries and one aorta, obtained from organ donors without history of cardiovascular disease. All human samples were collected with informed consent from patients; all studies were approved by the regional Ethical Committee and follow the guidelines of the Declaration of Helsinki.

Microarray dataset analyses were performed with GraphPad Prism 6 and Bioconductor software using a linear regression model adjusted for age and gender or a two-sided Student's t-

test assuming non-equal deviation, with correction for multiple comparisons according to Bonferroni, as previously described (8). In all analyses $p<0.05$ was considered to indicate statistical significance. The microarray dataset is available from Gene Expression Omnibus (GSE21545).

RNA in situ hybridization:

For in situ hybridization (ISH), we used a Qiagen miRCURY LNA DIG-labeled probe (5'-3' sequence:/5DigN/ATATTACTTTCCAATCAACTCA/3Dig_N/) with the accompanying kit and protocol (Qiagen, Venlo, The Netherlands). In brief, tissue sections were deparaffinized (formalin-fixed paraffin embedded) and rehydrated. Nucleases were inactivated with proteinase K followed by a 2 hr hybridization at hybridization temperature (64°C). Slides were washed in saline sodium citrate buffers with subsequent DIG detection methods. Nuclear counterstaining was performed with Nuclear Fast Red (Sigma Aldrich).

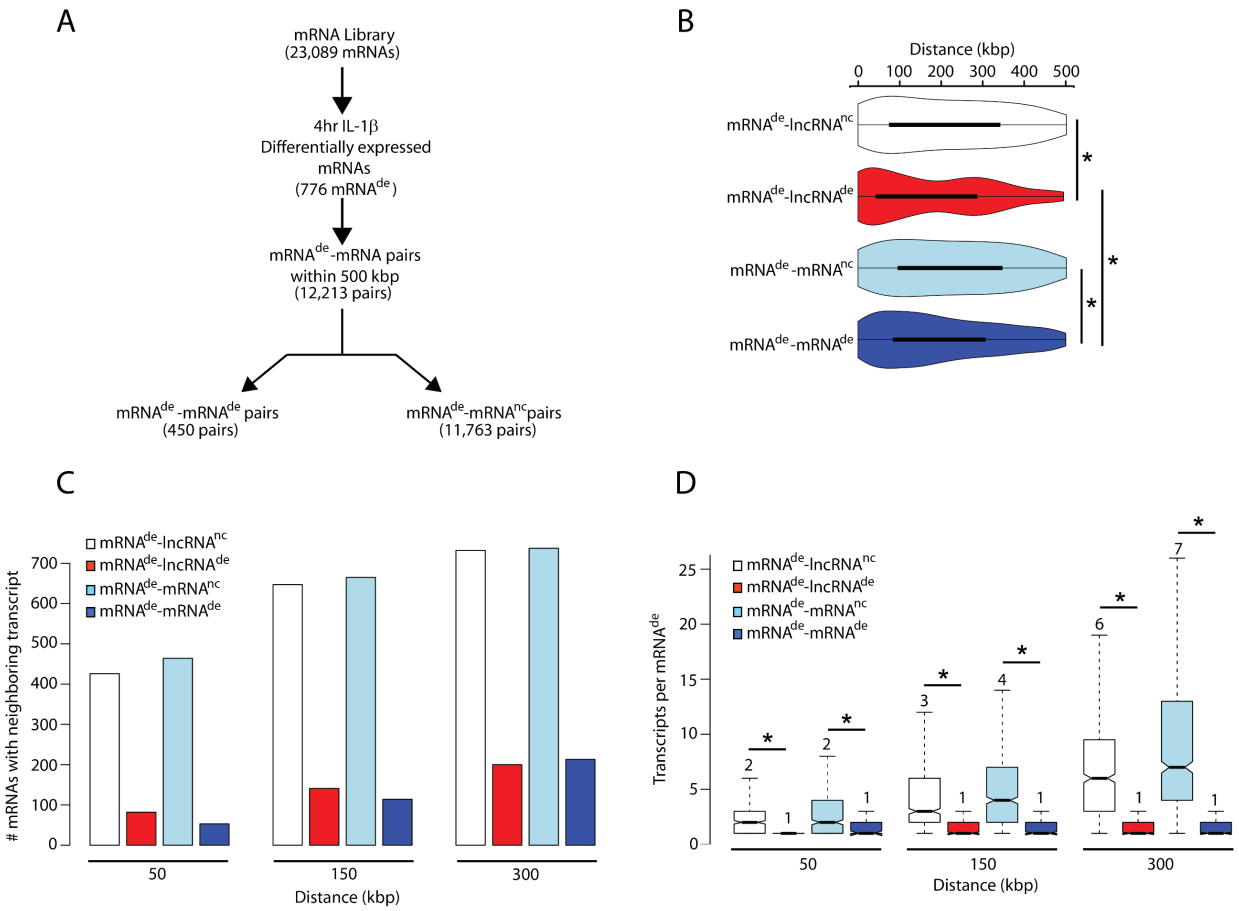

Supplementary Figure 1. Identification of IL-1β regulated mRNA-mRNA and mRNA-lncRNA neighboring pairs. A) Schematic of the computational pipeline used to identify neighboring mRNA-mRNA pairs, where the mRNAs are either IL-1β regulated ($mRNA^{de}$) or not ($mRNA^{nc}$). de = differentially expressed, nc = no change. B) Violin plots illustrating the distribution of genomic distance between transcript pairs. *p<0.02, Wilcoxon unpaired rank-sum test with Bonferroni correction. C) Bar graph showing the number of $mRNA^{de}$ that have a neighboring $mRNA^{de}$, $mRNA^{nc}$, $lncRNA^{de}$ or $lncRNA^{nc}$ transcript within the specified genomic distance. D) Box plots showing the number of neighboring $lncRNA^{nc}$, $lncRNA^{de}$, $mRNA^{nc}$, and $mRNA^{de}$ per neighboring $mRNA^{de}$ that are within 50, 150, and 300 kbp. *p<0.05, Student's t-test with Bonferroni correction.

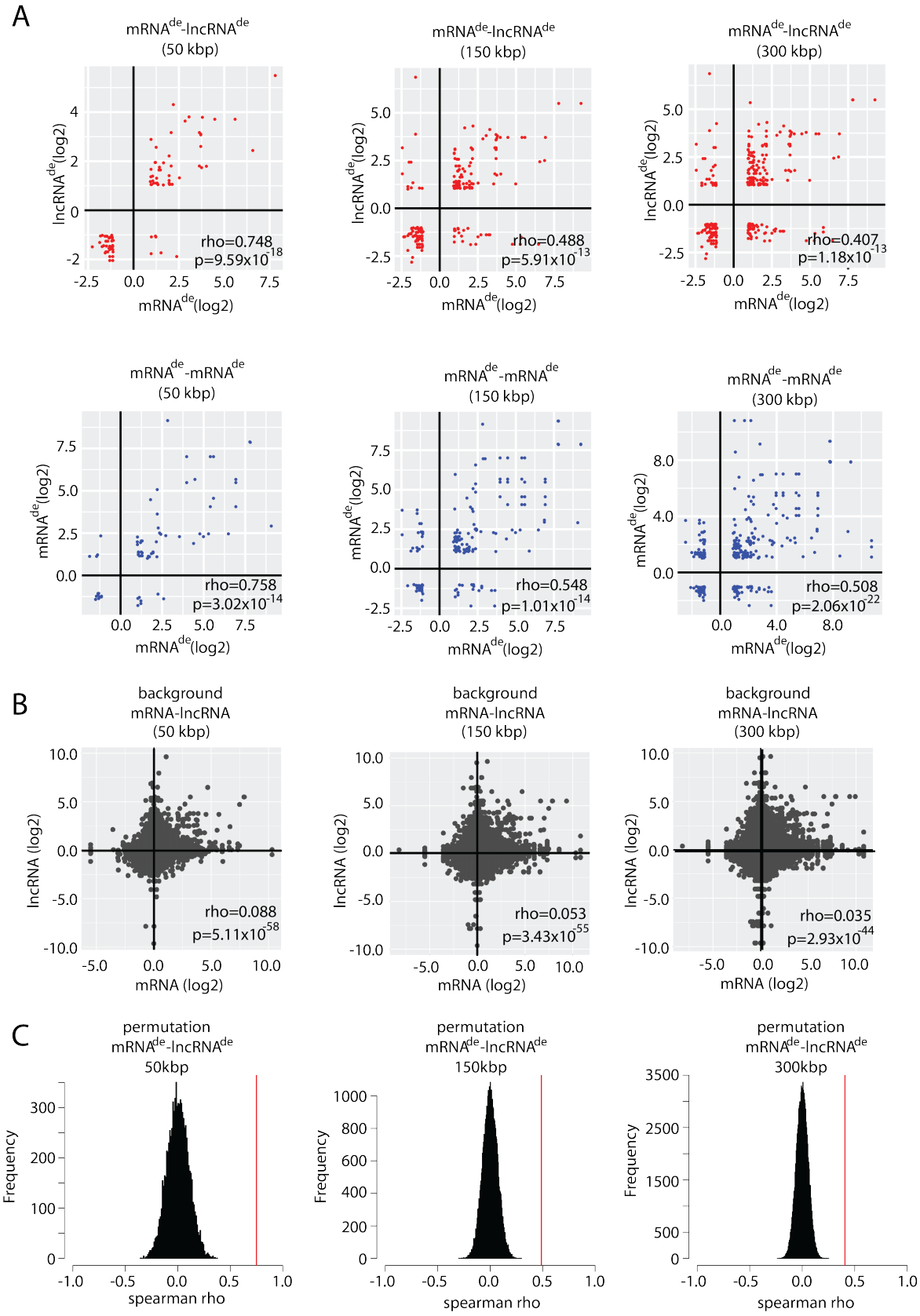
A
mRNA^de-lncRNA^de
(50 kbp)
lncRNA^de(log2)
mRNA^de(log2)
rho=0.748
p=9.59x10^-18
mRNA^de-lncRNA^de
(150 kbp)
rho=0.488
p=5.91x10^-13
mRNA^de-lncRNA^de
(300 kbp)
rho=0.407
p=1.18x10^-13
mRNA^de-mRNA^de
(50 kbp)
rho=0.758
p=3.02x10^-14
mRNA^de-mRNA^de
(150 kbp)
rho=0.548
p=1.01x10^-14
mRNA^de-mRNA^de
(300 kbp)
rho=0.508
p=2.06x10^-22
B
background
mRNA-lncRNA
(50 kbp)
lncRNA (log2)
mRNA (log2)
rho=0.088
p=5.11x10^-58
background
mRNA-lncRNA
(150 kbp)
rho=0.053
p=3.43x10^-55
background
mRNA-lncRNA
(300 kbp)
rho=0.035
p=2.93x10^-44
C
permutation
mRNA^de-lncRNA^de
50kbp
Frequency
spearman rho
permutation
mRNA^de-lncRNA^de
150kbp
permutation
mRNA^de-lncRNA^de
300kbp

Supplementary Figure 2. Correlation in expression of mRNA^{de}-lncRNA^{de} and mRNA^{de}-mRNA^{de} neighboring pairs. A) Scatterplots showing the log2 fold changes of mRNA^{de} on the x-axis and the log2 fold changes of their neighboring lncRNA^{de} (top) or mRNA^{de} (bottom) on the y-axis. Spearman rho correlation coefficient and its associated p-values are indicated. B) Scatterplots showing the log2 fold changes of all mRNAs on the x-axis and the log2 fold changes of all lncRNAs on the y-axis for a given genomic distance. Spearman rho correlation coefficients and their associated p-values are indicated. C) Histograms showing the distribution of spearman rho values calculated from randomized mRNA^{de}-lncRNA^{de} pairs that are not neighboring each other. The vertical red line represents the spearman rho value calculated from the neighboring mRNA^{de}-lncRNA^{de} data set.

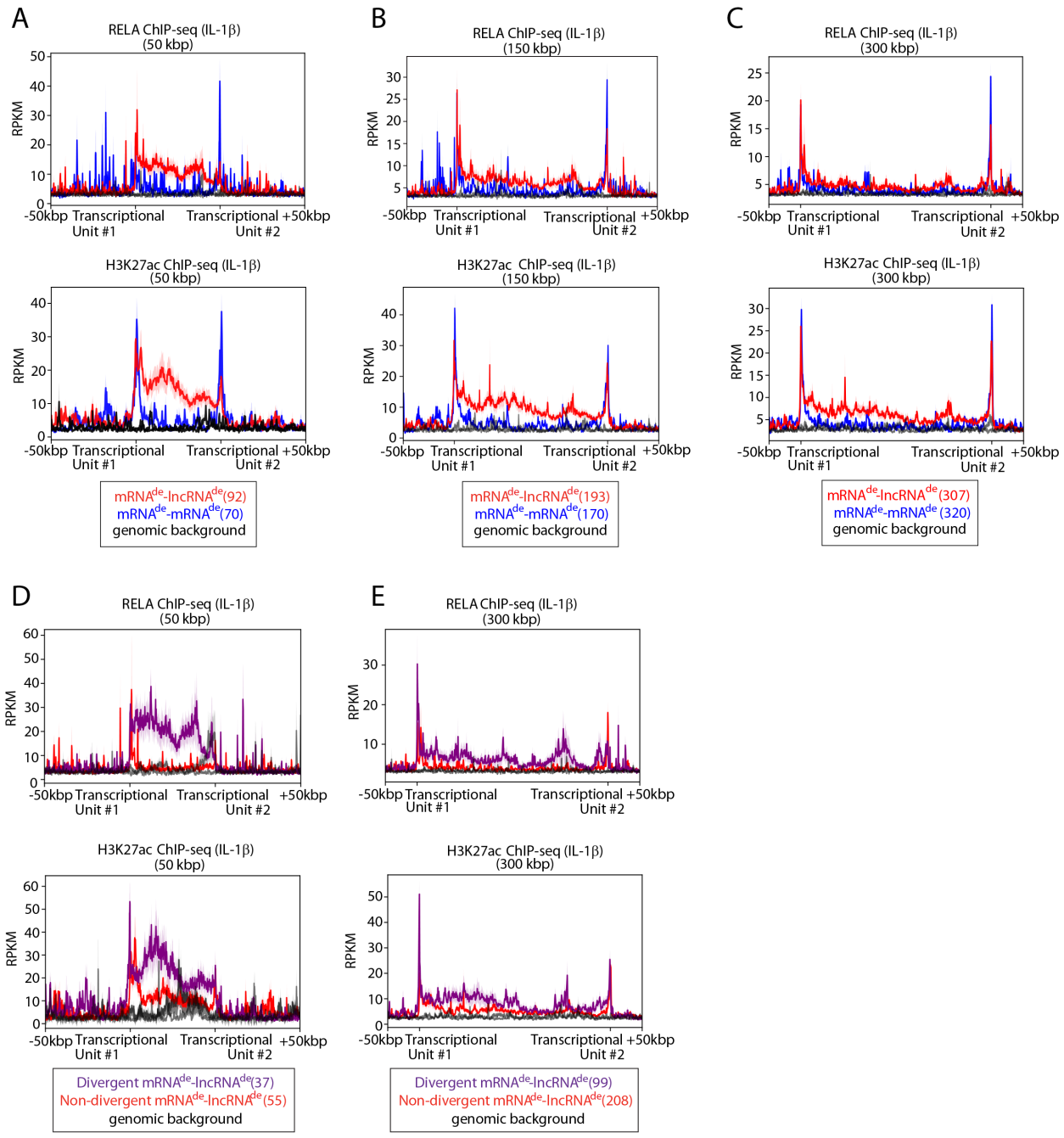

Supplementary Figure 3. Divergent mRNA^{de}-lncRNA^{de} pairs have shared regulatory elements. A-C) Profile plot of RELA and H3K27ac ChIP-seq signals in IL-1β treated cells for the region between the transcriptional start site (TSS) of an mRNA^{de} and the TSS of its neighboring lncRNA^{de} or mRNA^{de} transcript. Shown are neighboring pairs within 50 kbp (A), 150 kbp (B) or

300 kbp (C) of each other. The number of transcripts in each category is indicated in brackets. D-E) Profile plot of RELA and H3K27ac ChIP-seq signals in IL-1β treated cells for regions between the TSS of $mRNA^{de}$-$lncRNA^{de}$ pairs that either are or are not divergently transcribed. Shown are neighboring pairs within 50 kbp (D) or 300 kbp (E) of each other. The number of transcripts in each category is indicated in brackets.

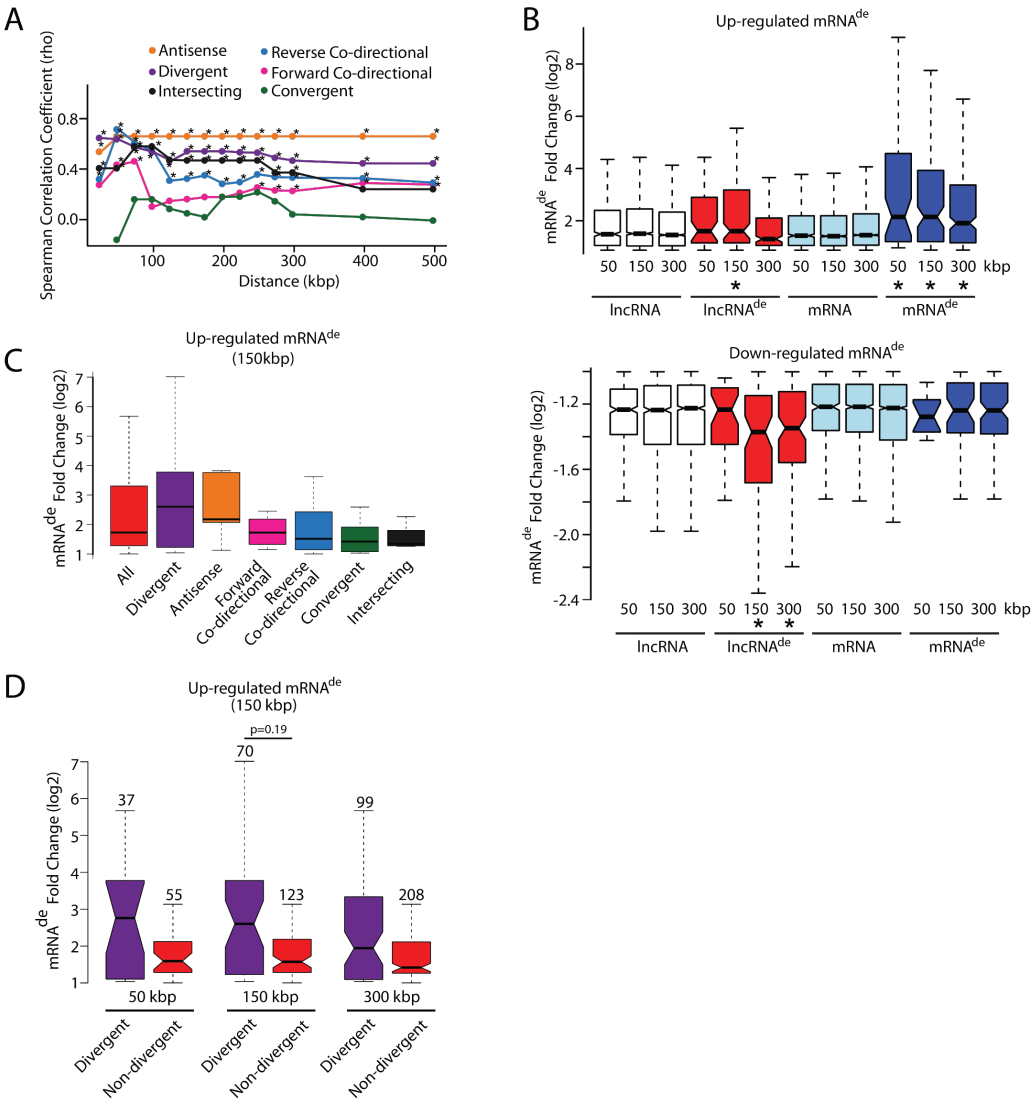

Supplementary Figure 4. Divergent and antisense mRNA^{de}-lncRNA^{de} pairs tend to have higher correlation and mRNA^{de} up-regulation than those transcribed in other orientations.

A) Spearman rho correlation coefficient for mRNA^{de}-lncRNA^{de} pairs depending on type of transcriptional orientation. *p<0.05, significance associated with each spearman's rho correlation coefficient. B) Box plots displaying the log2 fold change of up-regulated or down-regulated mRNA^{de} that have a neighboring mRNA^{nc}, mRNA^{de}, lncRNA^{nc} or lncRNA^{de}. *p<0.05, Wilcoxon unpaired rank-sum test with Bonferroni correction, lncRNA^{nc} vs lncRNA^{de} or mRNA^{nc} vs

mRNA^{de}. C) Box plots displaying the log2 fold change of up-regulated mRNA^{de} depending on its transcriptional orientation to its neighboring lncRNA^{de}. D) Box plots displaying the log2 fold change of up-regulated mRNA^{de} based on whether it is neighboring a divergent or non-divergent lncRNA^{de}. The number of observations in each group are shown above each boxplot. Wilcoxon unpaired rank-sum test with Bonferroni correction.

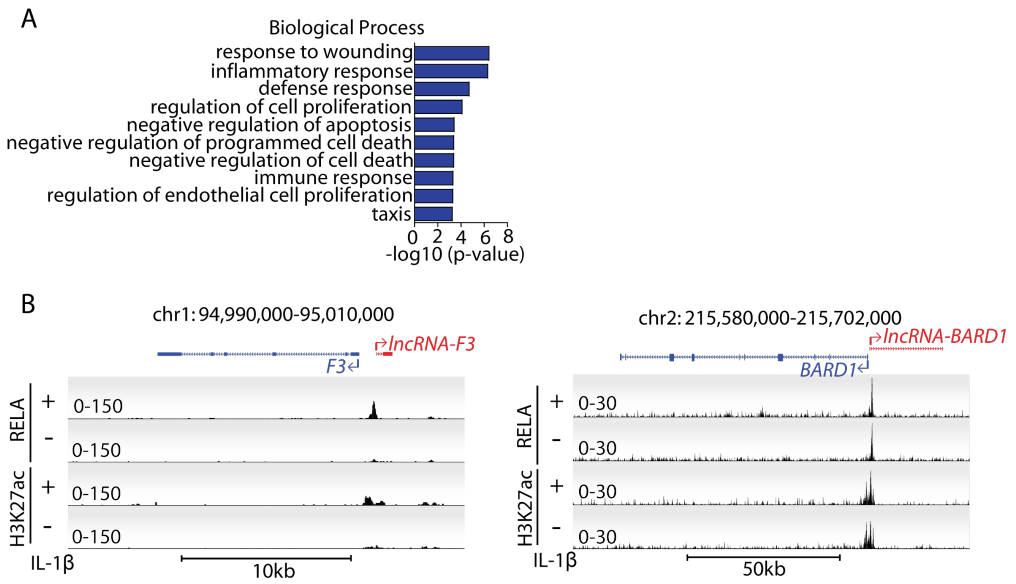

Supplementary Figure 5. Identification and characterization of divergent mRNA^{de}-lncRNA^{de} pairs. A) GO terms associated with the mRNAs from the indicated divergent mRNA^{de}-lncRNA^{de} pairs. B) UCSC genome browser tracks depicting *lncRNA-F3* and *lncRNA-BARD1* ChIP-seq tracks are shown for RELA and H3K27ac under either basal conditions or upon IL-1β treatment.

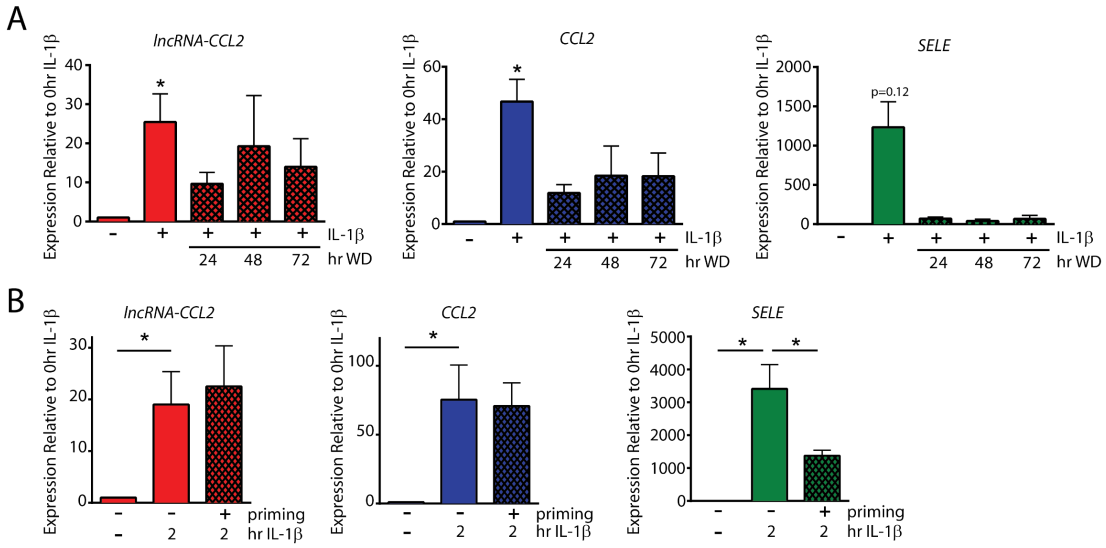

Supplementary Figure 6. *CCL2* and *lncRNA-CCL2* show coordinated expression in response to withdrawal and re-stimulation with IL-1β. A) qRT-PCR data showing expression kinetics of *lncRNA-CCL2*, *CCL2,* and *SELE* in HUVEC that were stimulated with IL-1β for 24 hours, followed by withdrawal of IL-1β for 24-72 hours. *p<0.05, Friedman test with Dunn's multiple comparisons test, relative to basal, n=4. B) qRT-PCR data showing expression of *lncRNA-CCL2*, *CCL2,* and *SELE* in HUVECs that were stimulated with IL-1β for 24 hours, followed by withdrawal of IL-1β for 24 hours and then re-stimulation with IL-1β for 2 hours. *p<0.05, paired student t-test, n=7-9.

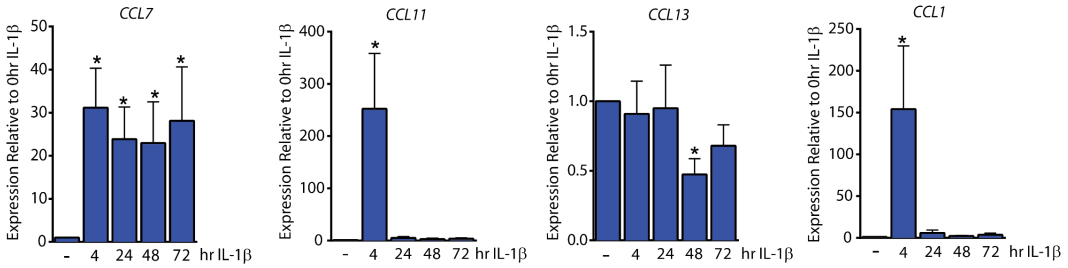

Supplementary Figure 7. Other *CCL* loci genes do not show coordinated IL-1β mediated expression with *lncRNA-CCL2*. qRT-PCR data showing the expression of *CCL7*, *CCL11*, *CCL8, CCL13*, and *CCL1* upon 4 to 72-hour treatment with IL-1β. *p<0.05, Friedman test with Dunn's multiple comparisons test, relative to basal, n=6.

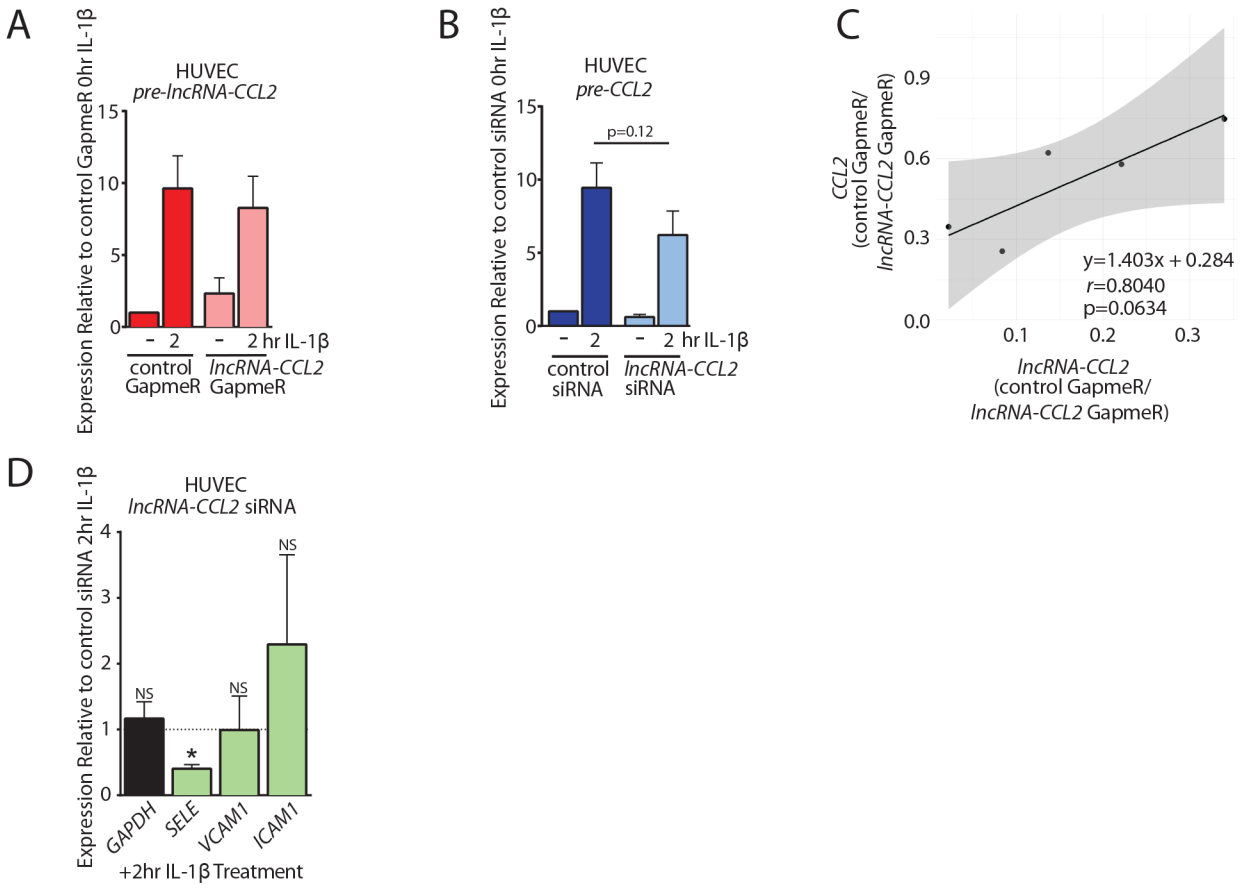

Supplementary Figure 8. *lncRNA-CCL2* positively regulates levels of its neighboring *CCL2* gene. A) qRT-PCR data of *pre-lncRNA-CCL2* (qRT-PCR primers targeting intron 1) levels upon knockdown of *lncRNA-CCL2* using GapmeR under basal condition and upon stimulation with IL-1β for 2 hours in HUVEC. Paired student t-test, n=3. B) qRT-PCR data of *pre-CCL2* gene expression upon knockdown of *lncRNA-CCL2* using siRNA under basal condition and upon stimulation with IL-1β for 2 hours in HUVEC. Paired student t-test, n=4. There was a trend towards decreased *pre-CCL2* expression. C) Scatterplot showing the degree of *lncRNA-CCL2* knockdown using GapmeR in HMEC1 on the x-axis and decrease in *CCL2* mRNA on the y-axis. Line of best fit is added to show the positive linear relationship. The pearson correlation coefficient (*r*) and its associated p-value are shown. D) qRT-PCR data of inflammatory genes

upon knockdown of *lncRNA-CCL2* using siRNA and stimulation with IL-1β for 2 hours in HUVEC. *$p<0.05$, paired student t-test, n=3, NS=non-significant.

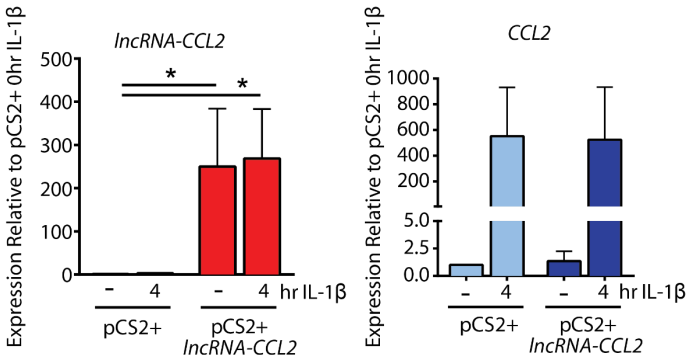

Supplementary Figure 9. *lncRNA-CCL2* overexpression does not result in change in *CCL2* levels. qRT-PCR data showing expression of *lncRNA-CCL2* and *CCL2* upon overexpression of spliced *lncRNA-CCL2* under basal conditions or upon 4 hours of IL-1β stimulation. *p<0.05, paired student t-test, n=3.

A

Result for species name : hg19 with job ID :1549419365							
Data ID	Sequence Name	RNA Size	ORF Size	Ficket Score	Hexamer Score	Coding Probability	Coding Label
0	LNCRNA_CCL2	341	87	0.7137	-0.176729382124	0.0022346814191944	no

B

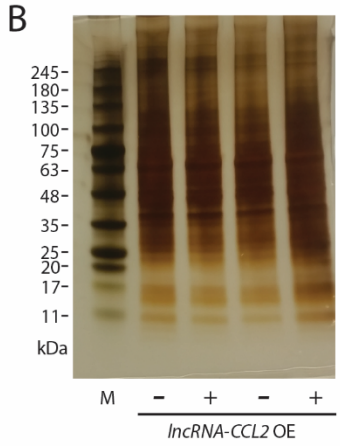

Supplementary Figure 10. *lncRNA-CCL2* does not appear to encode for a protein. A) Screenshot of the results of the CPAT (Coding-Potential Assessment Tool) program showing that *lncRNA-CCL2* is not predicted to encode for a protein. B) Silver stained SDS-PAGE gel showing total protein in HUVECs that either did or did not have *lncRNA-CCL2* overexpressed. M= protein ladder marker. No major changes in proteins were noted.

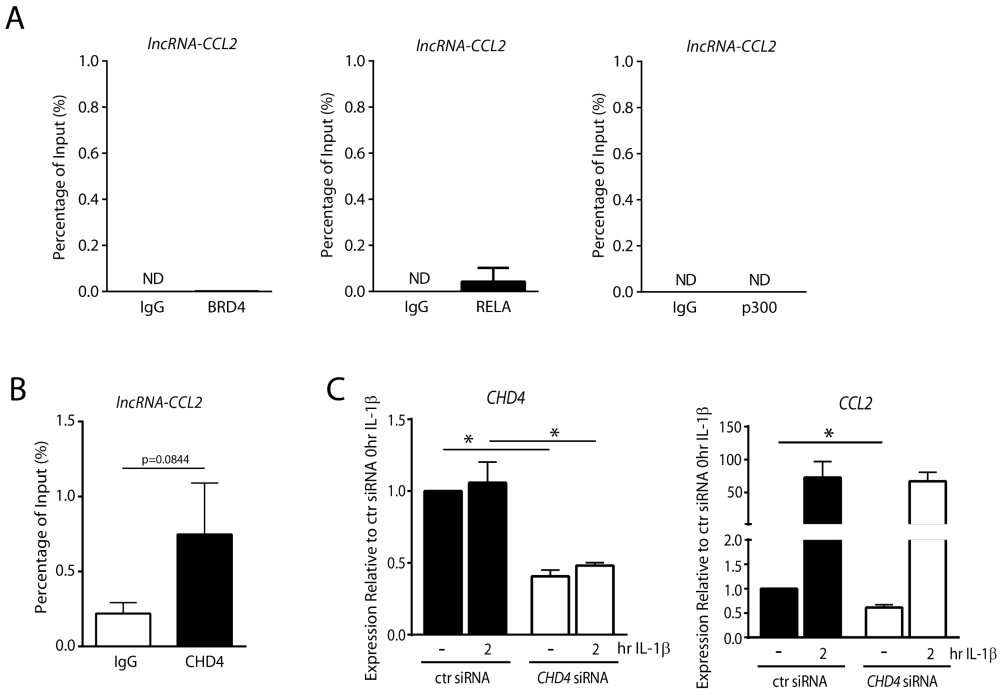

Supplementary Figure 11. *lncRNA-CCL2* regulation of *CCL2* levels is not due to interaction with chromatin machinery. A) Immunoprecipitation of BRD4, RELA, p300 or IgG control and detection of *lncRNA-CCL2* levels using qRT-PCR. ND = not detected. n=1, 2, and 2, respectively. B) Immunoprecipitation of CHD4 and detection of *lncRNA-CCL2* levels using qRT-PCR. Paired student t-test, n=3. C) qRT-PCR data of *CHD4*, *lncRNA-CCL2*, and *CCL2* expression upon knockdown of *CHD4* using siRNA under basal and 2-hour IL-1β stimulated conditions in HMEC1. *p<0.05, paired student t-test, n=3.

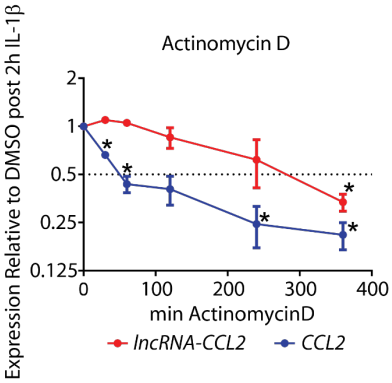

Supplementary Figure 12. *lncRNA-CCL2* and *CCL2* transcripts differ in their half-lives.

qRT-PCR data of *lncRNA-CCL2* and *CCL2* expression upon 2-hour IL-1β stimulation of HUVECs followed by Actinomycin D treatment for 0, 30, 60, 120, 240, or 360 minutes. Values are plotted as relative to DMSO treatment for equal length of time. *$p<0.05$, One way ANOVA with Dunnet multiple comparisons test, relative to 0 minutes Actinomycin D treatment, n=3.

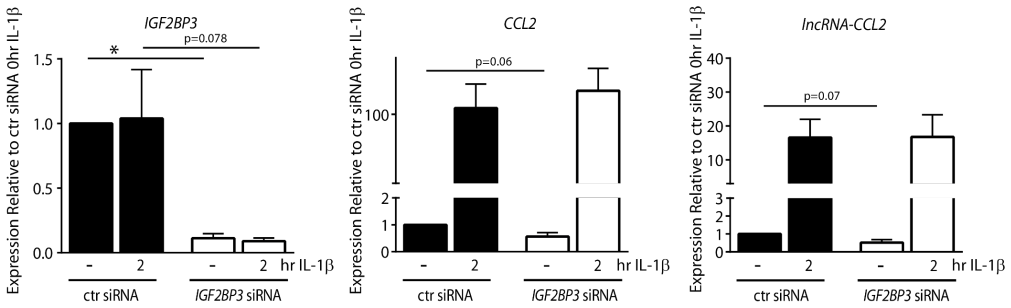

Supplementary Figure 13. *IGF2BP3* knockdown does not result in changes in *CCL2* levels.

qRT-PCR data of *IGF2BP3*, *CCL2*, and *lncRNA-CCL2* expression upon knockdown of *IGF2BP3* using siRNA under basal and 2-hour IL-1β stimulated conditions in HMEC1. *p<0.05, paired student t-test, n=4.

Supplementary Tables

Table S1. siRNA and GapmeR Sequences

Target	siRNA or GapmeR	ID#	Sequence (5'-->3')	Concentration
lncRNA-CCL2	siRNA	s500816	GGCAAAGCCACAUGGAUUAtt	20 nM
lncRNA-CCL2	GapmeR	300601-00	AGTTACTGAAGTGGCG	30 nM
CHD4	siRNA	S2985	CACUCGAAAUUUUGAAGCAtt	60 nM
HNRNPU	siRNA	S6743	CUACCUGGGUUACUAAACAtt	20 nM
IGF2BP2	siRNA	s20924	GAACUUAACCAGUGCAGAAtt	20 nM
IGF2BP3	siRNA	s20920	CUUUGUUAGUCCUAAAGAATT	20 nM

Table S2. Cloning primers and sequences of *lncRNA-CCL2* and scrambled control

lncRNA-CCL2	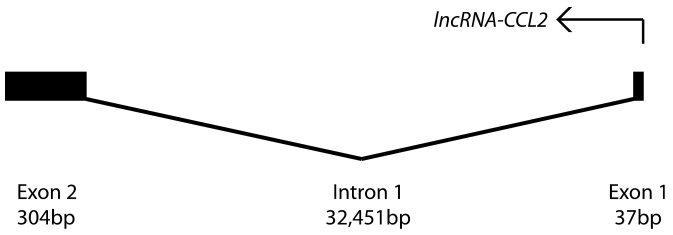
lncRNA-CCL2 Exon1 chr17:32578892-32578928	Cctgtttctctgatggggagactgaggccatgaacag
lncRNA-CCL2 Exon2 chr17:32546137-32546440	Atgaagaaacagacttaaagaagggaagtgacttggcaaagccacatggattaaaagggttga Agccaagaacaaaagcttggaagtcagaggagtctgctccctccactgtattgggttctctatcta Caagcagaggagcctgaagaaggaatgagttgattggaaagtaatatgttccctgttattgaagg Tgaccacctgtcaatgattccatggaaaagactcaagaaaaacaaattggtagatctttggagtta ggatcttagactctaaaatcatacgccacttcagtaactcattg
lncRNA-CCL2 Forward Cloning Primer - BamHI	CATGGATCCTGTTTCTCTGATGGG BamHI Site
lncRNA-CCL2 Reverse Cloning Primer - XbaI	CATTCTAGACAATGAGTTACTGAAG XbaI Site
lncRNA-CCL2	cctgtttctctgatggggagactgaggccatgaacagatgaagaaacagacttaaagaag ggaagtgacttggcaaagccacatggattaaaagggttgaagccaagaacaaaagcttgg aagtcagaggagtctgctccctccactgtattgggttctctatctacaagcagaggagcc tgaagaaggaatgagttgattggaaagtaatatgttccctgttattgaaggtgaccacct gtcaatgattccatggaaaagactcaagaaaaacaaattggtagatctttggagttagga tcttagactctaaaatcatacgccacttcagtaactcattg
Scrambled lncRNA	Ttatattctagacaatgagttactgaagtggcgtatgattttagagtctaagatcctaac tccaaagatctaccaatttgtttttcttgagtcttttccatggaatcattgacaggtggt caccttcaataacagggaacatattactttccaatcaactcattccttcttcaggctcct ctgcttgtagatagagaacccaatacagtggagggagcagactcctctgacttccaagct tttgttcttggcttcaacccttttaatccatgtggctttccgcctctcgacaatttcttt aagtctgtttcttcatctgttcatggcctcagtctccccatcagagaaacaggggatcctat

Table S3. mRNA validation primers

mRNA Name	**mRNA Symbol**	**Primer F**	**Primer R**
OSGIN2	NM_001126111	TGGAAGTTGGATGGAACTACCTG	TTTCCTCTGGCATAACTCGATCC
NR2F2	NM_001145155	ACATACGGATCTTCCAAGAGCAA	CTTTTCCTGCAAGCTTTCCACAT
MEIS2	NM_170675	GACACATCCAGGAGTTTATTGGA	GAGGGTCTCCGTACATGGAA
BARD1	NM_000465	TTGCTGCTACCAGAGAAGAATG	GTACAAGAGGTCCATCCCTACG
TNFAIP6	NM_007115	CAATAGGAGTGAAAGATGGGATG	GTGCCAGTAGCAGATTTGGTTAT
IER5L	NM_203434	ATACCCTACCCCTTCGGACTT	TCACCACGTGAGTGTCTAGGTC
CLEC14A	NM_175060	TTGGGGAAGCCAGCTGTA	GCTCCCAACTTGGATCTGTC
F3	NM_001178096	AGTTCACACCTTACCTGGAGACA	GGCTTAGGAAAGTGTTGTTCCTT
CAV2	NM_001206747	ATGTACAAGTTCCTGACGGTGTT	CAGAACCATTAGGCAGGTCTTTA
IL15	NM_000585	GAGTCCGGAGATGCAAGTATTC	GCATCCAGATTCTGTTACATTCC
HES1	NM_005524	GACATTCTGGAAATGACAGTGAAG	GTCACCTCGTTCATGCACTC
MESDC1	NM_022566	ATCTCAGGCTTTAAGGGAGAGG	TATAAATGGAGAGGGGCAGAGA
DACH1	ENST00000313174	GAGACCCTCTACAATGACTGCAC	GAATTATCCCAGGAGACATGAGA
C8orf4	NM_020130	GAAACTCTGGAGACAAGAAAGCA	CTCCTCCACATCTTGATCTATGG
SLC2A1	NM_006516	AATGCTGATGATGAACCTGCT	AGGATCAGCATCTCAAAGGACT
RIPK2	NM_003821	GAAGCACCTGCACATCCAC	AGGCTCATTGCAAATTCCCA
SMAD3	NM_001145104	ATGTCAACAGGAATGCAGCAGTGG	ATAGCGCTGGTTACAGTTGGGAGA
CCL2	NM_002982	GCTCAGCCAGATGCAATCAA	TTCTTTGGGACACTTGCTGC
CCL7	NM_006273	CAGAGGCTGGAGAGCTACAG	GATTACAGCTTCCCGGGGAC
CCL11	NM_002986	TCCAACATGAAGGTCTCCGC	TCTCTAGTCGCTGAAGGGGT
CCL8	NM_005623	TGGAGAGCTACACAAGAATCACC	TGGTCCAGATGCTTCATGGAA
CCL13	ENST00000225844	CTTGCAGAGGCTGAAGAGCT	GATGACAGCCTTCTGGGGAC

Table S4. lncRNA validation primers.

lncRNA Name	**lncRNA Symbol**	**Primer F**	**Primer R**
lncRNA-OSGIN2/RIPK2	ENST00000523859	CCTTGAGAGAGTCCATCCATCTA	GAGGCAGAAGAATTGCTTGAA
lncRNA-NR2F2	ENST00000560010	GTTGGACCGTACTCGGATCT	CTTGTGAAGATGTTGCATACAGG
lncRNA-NR2F2-2	ENST00000561402	GAGGTGAAACAAACTGGGTTATG	TCTGAACATGATGCCAAACAC
lncRNA-BARD1	TCONS_00004010	GTTTTGACTGCTGTTGGACTTG	GGCAGCTAATTACGCTTCAGTAT
lncRNA-SMAD3	ENST00000558436	CCATCATGACTGCTATTGGAAA	AATCCCACCTCTAGGAAACTCC
lncRNA-IER5L	uc010myu.1	CGTCTGGCTCTCCAACTAGACT	CAGTGGCTACATCCACTCTCTG
lncRNA-CLEC14A	ENST00000555636	AGGAAAAGAATGCAGACACCTC	GAAGTTGCCATATGAATGCTACC
lncRNA-F3	TCONS_00001037	CAGCTTAGGTCTGAGGGTCAGT	CCTCAGTCACTATCTCTGGTCGT
lncRNA-CAV2	ENST00000439070	CAAATGGCACTCATTAAGGACA	GTGCTGCTCTCAGTAGCAAGTTA
lncRNA-IL15	ENST00000509161	AGAGGAGAAAAGTGGCAGACAG	GTCCATGAGGTAGATGCAATCA
lncRNA-HES1	NR_033944	TGGGGAGAACTTATAAGAGTTTGG	CCCCTTCTCCTCTTTTTCATTT
lncRNA-HES1-2	ENST00000418353	GAGGGCTATTGAACGAGCTTT	CTGGAATGTGCTGTTTCTGG
lncRNA-MESDC1	ENST00000563737	TGAATCACTTAGAGGTGGGGTTA	CAGATGTGAAAGATTGTGTGCTC
lncRNA-DACH1	uc.353+	GAGGACAAGTTTGGTAGACCTGA	GCATCCAGGTTATTGTTCATTG
lncRNA-C8orf4	TCONS_00014982	TAGGCTATGTGAACCGTCACTG	TCAGGGGAGAGTAAAGACAAGC
lncRNA-CCL2/ CCL7/ CCL8/ CCL13	TCONS_00025610	GGGAGACTGAGGCCATGAAC	GCTTTGCCAAGTCACTTCCC

Table S5. qPCR primers

Transcript Name	**Transcript Symbol**	**Primer F**	**Primer R**
TBP	NM_003194	TCGGAGAGTTCTGGGATTGT	CACGAAGTGCAATGGTCTTT
GAPDH	NM_002046	AGGTGAAGGTCGGAGTCAAC	GAGGTCAATGAAGGGGTCAT
CCL2	NM_002982	GCTCAGCCAGATGCAATCAA	TTCTTTGGGACACTTGCTGC
CCL7	NM_006273	CAGAGGCTGGAGAGCTACAG	GATTACAGCTTCCCGGGGAC
CCL11	NM_002986	TCCAACATGAAGGTCTCCGC	TCTCTAGTCGCTGAAGGGGT
CCL8	NM_005623	TGGAGAGCTACACAAGAATCACC	TGGTCCAGATGCTTCATGGAA
CCL13	NM_005408	CTTGCAGAGGCTGAAGAGCT	GATGACAGCCTTCTGGGGAC
CCL1	NM_002981	ATACCAGCTCCATCTGCTCC	TTCTGTGCCTCTGAACCCAT
SELE	NM_000450	GAACCAAAGACTCGGGCATGT	ATGACCACTGCAGGATGCATT
VCAM1	NM_001078	GTTGAAGGATGCGGGAGTAT	GGATGCAAAATAGAGCACGA
ICAM1	NM_000201	CGGCCAGCTTATACACAAGA	GTCTGCTGGGAATTTTCTGG
lncRNA-CCL2 (exon 1- exon 2)	TCONS_00025610	GGGAGACTGAGGCCATGAAC	GCTTTGCCAAGTCACTTCCC
pre-lncRNA-CCL2 (intron 1)	TCONS_00025610	GGTCTTTACAACAGCCTGCC	TATGTGGCCCTGGTCAAAGT
pre-CCL2 (intron 1)	NM_002982	TGAACCCCAAATCCAGCTCC	GGAGTAACTGCGCTGAGTGT
CHD4	NM_001297553	GGAGCCTAAATCATCTGCTCAG	GTGAGGGTTCGATAATCCTCCT
HNRNPU	NM_004501	GAGCATCCTATGGTGTGTCAAA	TGACCAGCCAATACGAACTTC
IGF2BP2	NM_001007225	AGAACTTAACCAGTGCAGAAGTCAT	CCTGTTGTACAATTTCCCTGATCT
IGF2BP3	NM_006547	AATAACTGGTCACTTCTATGCTTGC	GCTGCTTTACCTGAGTCAGAATTT
MT-CO2	YP_003024029	ACGCATCCTTTACATAACAGAC	GCCAATTGATTTGATGGTAAGG
MALAT1	NR_002819	GTGATGCGAGTTGTTCTCCG	CTGGCTGCCTCAATGCCTAC

Table S6. ChIP-seq Quality Control Metrics for GEO: GSE89970 (1).

GEO Dataset	Name	# Raw Reads	# Mapped Reads	% Mapped Reads
GSM2394419	HAEC.ChIP.p65.control.4h.rep1	21152400	20606203	97.42
GSM2394420	HAEC.ChIP.p65.control.4h.rep2	28442645	27682692	97.33
GSM2394421	HAEC.ChIP.p65.IL1b.4h.rep1	26751263	25743447	96.23
GSM2394422	HAEC.ChIP.p65.IL1b.4h.rep2	38346553	37207429	97.03
GSM2394402	HAEC.ChIP.H3K27ac.control.4h.rep1	29804176	29420670	98.71
GSM2394403	HAEC.ChIP.H3K27ac.control.4h.rep2	22993877	22761469	98.99
GSM2394404	HAEC.ChIP.H3K27ac.IL1b.4h.rep1	20663461	20318255	98.33
GSM2394405	HAEC.ChIP.H3K27ac.IL1b.4h.rep2	31291354	31043431	99.21
GSM2394425	HAEC.input.control.4h.DSG	22962769	22535711	98.14
GSM2394426	HAEC.input.control.4h.formaldehyde	13642816	13407807	98.28
GSM2394427	HAEC.input.IL1b.4h.DSG	32367536	31768065	98.15
GSM2394428	HAEC.input.IL1b.4h.formaldehyde	19810556	19455987	98.21

GEO Dataset	# Uniquely Mapped Reads	% Uniquely Mapped Reads	# of Peaks	PBC	NRF (Library Size Adjusted)	NSC	RSC
GSM2394419	15787670	74.64	3594	0.54	0.725	1.171	1.163
GSM2394420	21174704	74.45	31866	0.699	0.863	1.276	1.357
GSM2394421	20623464	77.09	53766	0.273	0.55	2.114	1.943
GSM2394422	28621202	74.64	53548	0.397	0.731	1.606	1.787
GSM2394402	24317915	81.59	68514	0.361	0.681	1.719	1.563
GSM2394403	18712945	81.38	55165	0.895	0.886	1.974	1.337
GSM2394404	16354165	79.15	33847	0.213	0.326	1.792	1.292
GSM2394405	26467892	84.59	74091	0.835	0.924	2.486	1.367
GSM2394425	16800910	73.17	NA	0.95	0.952	1.029	0.321
GSM2394426	10186183	74.66	NA	0.903	0.91	1.08	0.515
GSM2394427	23501019	72.61	NA	0.961	0.963	1.018	0.295
GSM2394428	14951618	75.47	NA	0.937	0.951	1.041	0.486

Supplementary Datasets

Dataset S1- Arraystar Microarray Results

- Sheet 1- Raw Data- lncRNA microarray
- Sheet 2- Raw Data- mRNA microarray
- Sheet 3- lncRNA microarray results
- Sheet 4- mRNA microarray results

Dataset S2- Differentially Expressed mRNAs and lncRNAs

- Sheet 1- lncRNA- IL1B de (differentially expressed) 4 hr
- Sheet 2- mRNA- IL1B de (differentially expressed) 4 hr
- Sheet 3- lncRNA- IL1B de (differentially expressed) 24 hr
- Sheet 4- mRNA- IL1B de (differentially expressed) 24 hr

Dataset S3- Neighboring $mRNA^{de}$-$lncRNA^{de}$ and $mRNA^{de}$-$mRNA^{de}$

- Sheet 1- 50kbp $mRNA^{de}$-$lncRNA^{de}$
- Sheet 2- 150kbp $mRNA^{de}$-$lncRNA^{de}$
- Sheet 3- 300kbp $mRNA^{de}$-$lncRNA^{de}$
- Sheet 4- 50kbp $mRNA^{de}$-$mRNA^{de}$
- Sheet 5- 150kbp $mRNA^{de}$-$mRNA^{de}$
- Sheet 6- 300kbp $mRNA^{de}$-$mRNA^{de}$
- Sheet 7- pairs tabulation

Dataset S4- Spearman Correlation

- Sheet 1- Genomic distance correlation
- Sheet 2- TAD correlation

Dataset S5- Transcriptional Orientation Classification

- Sheet 1- $mRNA^{de}$-$lncRNA^{de}$ classification
- Sheet 2- $mRNA^{de}$-$mRNA^{de}$ classification
- Sheet 3- all classifications ($mRNA^{de}$-$lncRNA^{de}$) correlation
- Sheet 4- divergent ($mRNA^{de}$-$lncRNA^{de}$) correlation

Dataset S6- Same TAD Divergent $mRNA^{de}$-$lncRNA^{de}$ Pairs

- Sheet 1- Top $mRNA^{de}$-$lncRNA^{de}$ pairs
- Sheet 2- lncRNA info
- Sheet 3- mRNA info

Dataset S7- *lncRNA-CCL2* RNA-IP Mass Spectrometry Results

Citations:

1. Hogan NT*, et al.* (2017) Transcriptional networks specifying homeostatic and inflammatory programs of gene expression in human aortic endothelial cells. *eLife* 6.
2. Blankenberg D*, et al.* (2010) Manipulation of FASTQ data with Galaxy. *Bioinformatics* 26(14):1783-1785.
3. Langmead B & Salzberg SL (2012) Fast gapped-read alignment with Bowtie 2. *Nature Methods* 9(4):357.
4. Feng J, Liu T, Qin B, Zhang Y, & Liu X (2012) Identifying ChIP-seq enrichment using MACS. *Nature Protocols* 7(9):1728.
5. Barnett DW, Garrison EK, Quinlan AR, Strömberg MP, & Marth GT (2011) BamTools: a C++ API and toolkit for analyzing and managing BAM files. *Bioinformatics* 27(12):1691-1692.
6. Ramírez F*, et al.* (2016) deepTools2: a next generation web server for deep-sequencing data analysis. *Nucleic Acids Research* 44(W1).
7. Zhang Y*, et al.* (2016) Characterization of Long Noncoding RNA-Associated Proteins by RNA-Immunoprecipitation. *Methods in molecular biology (Clifton, N.J.)* 1402:19-26.
8. Naylor AR, Rothwell PM, & Bell PRF (2003) Overview of the principal results and secondary analyses from the European and North American randomised trials of endarterectomy for symptomatic carotid stenosis. *European Journal of Vascular and Endovascular Surgery* 26(2):115-129.
9. Perisic L*, et al.* (2016) Gene expression signatures, pathways and networks in carotid atherosclerosis. *Journal of Internal Medicine* 279(3):293-308.